JACS
JOURNAL OF THE AMERICAN CHEMICAL SOCIETY
pubs.acs.org/JACS
Article

Electrochemical Switching of a Fluorescent Molecular Rotor Embedded within a Bistable Rotaxane

Yilei Wu, Marco Frasconi,* Wei-Guang Liu, Ryan M. Young, William A. Goddard III, Michael R. Wasielewski,* and J. Fraser Stoddart*

Cite This: J. Am. Chem. Soc. 2020, 142, 11835−11846
Read Online
ACCESS | Metrics & More | Article Recommendations | Supporting Information

ABSTRACT: We report how the nanoconfined environment, introduced by the mechanical bonds within an electrochemically switchable bistable [2]rotaxane, controls the rotation of a fluorescent molecular rotor, namely, an 8-phenyl-substituted boron dipyrromethene (BODIPY). The electrochemical switching of the bistable [2]rotaxane induces changes in the ground-state coconformation and in the corresponding excited-state properties of the BODIPY rotor. In the starting redox state, when no external potential is applied, the cyclobis(paraquat-*p*-phenylene) ($CBPQT^{4+}$) ring component encircles the tetrathiafulvalene (TTF) unit on the dumbbell component, leaving the BODIPY rotor unhindered and exhibiting low fluorescence. Upon oxidation of the TTF unit to a TTF^{2+} dication, the $CBPQT^{4+}$ ring is forced toward the molecular rotor, leading to an increased energy barrier for the excited state to rotate the rotor into the state with a high nonradiative rate constant, resulting in an overall 3.4-fold fluorescence enhancement. On the other hand, when the solvent polarity is high enough to stabilize the excited charge-transfer state between the BODIPY rotor and the $CBPQT^{4+}$ ring, movement of the ring toward the BODIPY rotor produces an unexpectedly strong fluorescence signal decrease as the result of photoinduced electron transfer from the BODIPY rotor to the $CBPQT^{4+}$ ring. The nanoconfinement effect introduced by mechanical bonding can effectively lead to modulation of the physicochemical properties as observed in this bistable [2]rotaxane. On account of the straightforward synthetic strategy and the facile modulation of switchable electrochromic behavior, our approach could pave the way for the development of new stimuli-responsive materials based on mechanically interlocked molecules for future electro-optical applications, such as sensors, molecular memories, and molecular logic gates.

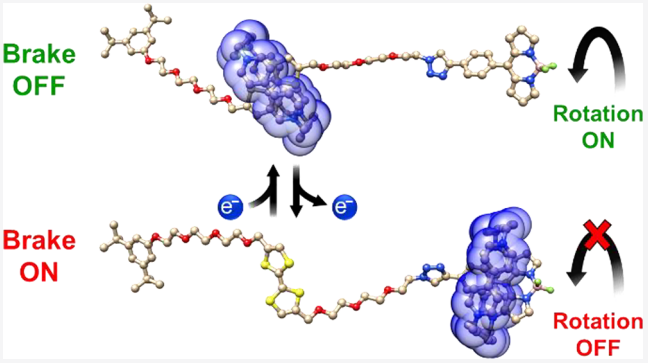

INTRODUCTION

Molecular devices and machines are of considerable interest on account of their potential use in sensing, catalytic, electronic, and nanotechnological applications.[1] Mechanically interlocked molecules (MIMs) constitute promising nanoscale molecular assemblies for the development of switches,[2] actuators,[3] ratchets,[4] and motors.[5] Well-known examples are bistable [2]rotaxanes,[2a,6] which are MIMs comprising a ring component mechanically bonded onto a linear dumbbell component with two (or more) recognition sites for occupation by the ring component. The ability to manipulate reversibly the relative positioning of the ring component with respect to the dumbbell component is crucial to exploring their use in operating molecular devices. Controlled rotary movement of a ring component around a dumbbell has been achieved[7] by introducing suitable steric hindrance between the two components of the rotaxane. On the other hand, the net linear translation of the ring with respect to a constitutionally asymmetric axle has been demonstrated in molecular shuttles[4b,c] and pseudorotaxanes[8] by exploiting ratchet mechanisms.[9] Recently, a rotaxane-based molecular shuttle, combined with an overcrowded alkene rotary motor, has led to transformation of the unidirectional rotation of the molecular motor into a reciprocating shuttling motion,[10] thus coupling rotary and translational movements in a MIM. Indeed, rotary motors are a class of molecular machines that display controlled rotation of one component with respect to the other around single[11] or double[12] bonds driven, for the most part, by either light or heat.

Fluorescent molecular rotors are compounds whose photoluminescence is modulated by segmental mobility (twisting), that is, the locally excited (LE) electronic state can relax either by (i) the radiative emission of a photon or by (ii) formation

Received: April 4, 2020
Published: May 29, 2020

https://dx.doi.org/10.1021/jacs.0c03701
J. Am. Chem. Soc. 2020, 142, 11835−11846

Scheme 1. (a) Covalent-Bond Approach to Enhancing the Fluorescence of BODIPY by Introducing Steric Constraints on the Aryl Ring and Dipyrrin Core, and Structure of the BODIPY Rotor Employed as a Viscosity-Sensitive Probe; (b) Mechanical-Bond Approach to Controlling the Rotation of the BODIPY Rotor by Redox Actuation of a Bistable [2]Rotaxane 6^{4+}[a]

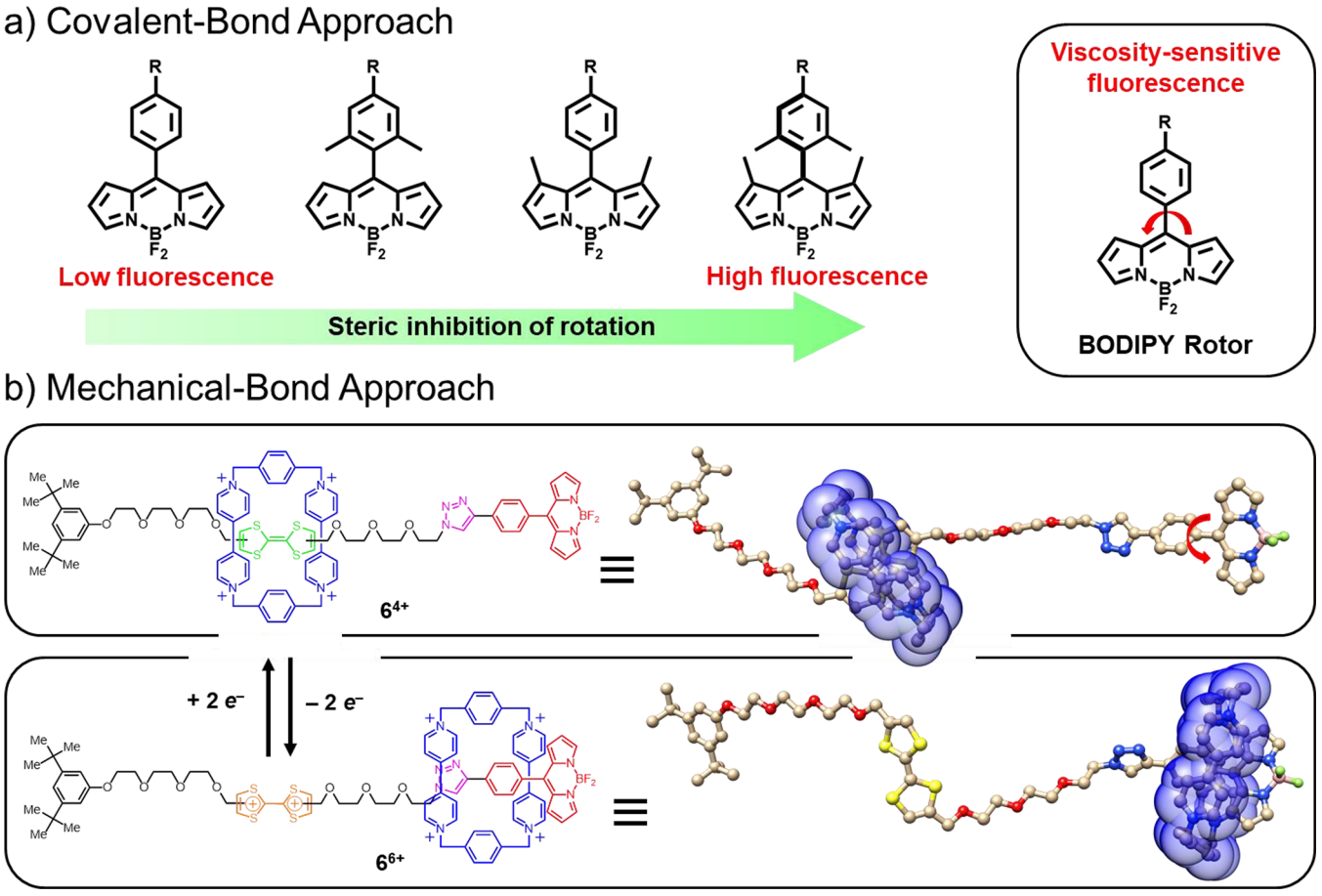

[a]Structural formulas and graphical representations of 6^{4+} and its redox switching from 6^{4+} to 6^{6+}.

of a "dark state" that relaxes nonradiatively to the ground state (GS) on account of internal rotation.[13] If the local environment around the fluorophore permits rapid rotation in the excited state, fast nonradiative decay processes can effectively quench its fluorescence. On the other hand, any environmental restriction to twisting in the excited state because of free volume, molecular crowding, or solvent viscosity slows down rotational relaxation, enhancing fluorescence efficiency from the LE state. This environmental sensitivity of fluorescent molecular rotors has been exploited[13] extensively in biological applications to probe, in real time, local microviscosity in biofluids and biomembranes.

One of the most widely used[14] fluorescent molecular rotors is (Scheme 1a) the BODIPY rotor. Introduction of steric constraints in the form of substituents onto the phenyl ring or the dipyrrin units of the BODIPY is an effective approach to increasing the quantum yield of these rotors by preventing free rotation of the phenyl group, thus reducing loss of energy from the excited states via nonradiative molecular motions.[15] Indeed, a theoretical study shows[15a] that the phenyl ring rotation and accompanying boron-dipyrrin distortions allow access to an excited-state conformation with low radiative probability and facile nonradiative deactivation to the ground state, thereby limiting the fluorescence yields of the dyes. Such a distorted conformation is energetically inaccessible in a system bearing the sterically hindered *o*-tolyl or mesityl group, leading to a high radiative probability, and high fluorescence quantum yield, involving conformations at or near the initial Franck–Condon form of the excited state.[15b] An increase in the fluorescence quantum yield of the BODIPY rotor is also observed[14] by increasing the solvent viscosity, which results in restricted rotation of the phenyl group, thus preventing nonradiative relaxation. This property of the BODIPY rotor and its derivatives has been employed successfully to measure viscosity in model lipid membranes,[16] in protocells,[17] and in the inner membranes of living cells.[18] One of the main advantages of the BODIPY rotor over other reported molecular rotors is the wide dynamic range of its fluorescence response,[14] corresponding to a broad range of viscosities, and a very weak sensitivity to solvent polarity[19] and temperature.[16] Control of the rotation of a fluorescent molecular rotor, imposed by mechanical bonds within the nanoconfinement[20] provided by a MIM, however, has not been explored so far to the best of our knowledge.

Herein, we designed (Scheme 1b) and synthesized a novel electrochemically switchable bistable [2]rotaxane (6^{4+}) with an embedded fluorescent rotor where the fluorescence output is actuated by an electrochemical stimulus. The bistable [2]-rotaxane (6^{4+}) is comprised of the π-electron-poor cyclobis-(paraquat-*p*-phenylene) $CBPQT^{4+}$ ring and a dumbbell containing a π-electron-rich tetrathiafulvalene (TTF) unit with a fluorescent BODIPY rotor acting as a stopper. This

https://dx.doi.org/10.1021/jacs.0c03701
J. Am. Chem. Soc. 2020, 142, 11835–11846

Scheme 2. Synthesis of the BODIPY-alkyne 4, the Bistable [2]Rotaxane 6·4PF$_6$, and the Dumbbell DB

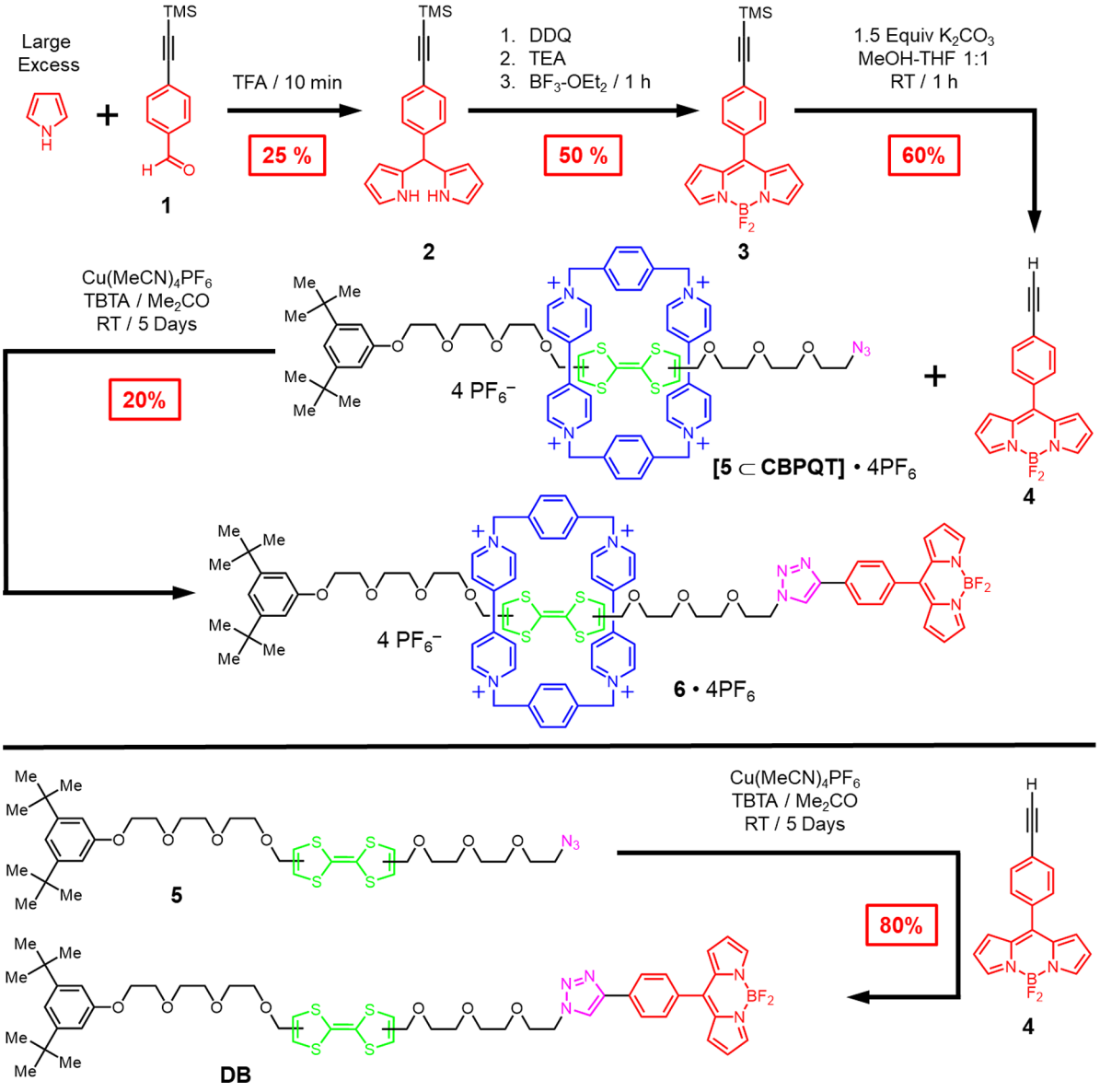

particular bistable [2]rotaxane has only one switchable recognition unit and therefore exists as a single translational coconformation in its ground state. Upon complete oxidation of the TTF unit to the stable, doubly charged TTF^{2+} dication, the CBPQT^{4+} ring is forced into juxtaposition with the BODIPY rotor as a result of Coulombic repulsions. The nature of the switching process has been investigated using (i) 1D and 2D NMR spectroscopies, (ii) steady-state and ultrafast time-resolved spectroscopies, (iii) electrochemical experiments, and (iv) quantum mechanical calculations. In low-polarity solvents, e.g., PhMe, oxidation of the TTF unit to a TTF^{2+} dication drives the CBPQT^{4+} ring toward the BODIPY rotor, increasing the fluorescence quantum yield of the latter. This remarkable fluorescence enhancement is a consequence of the increased energy barrier associated with its excited-state rotation which is responsible for its high nonradiative rate constant. The novelty of our approach lies in the ability to control the rotation of a molecular rotor by the constrained nanoconfined[20] environment introduced by the mechanical bonding associated with this electrochemically switchable bistable [2]rotaxane (Scheme 1b). The bistable [2]rotaxane can therefore be considered as a model electromechanical *molecular brake* based on Coulombic repulsion and actuated by redox inputs, where the coconformational change is readily monitored through the fluorescence output. On the other hand, in high-polarity solvents, e.g., MeCN, an excited charge-shifted (CS) state involving electron transfer from the BODIPY rotor to the CBPQT^{4+} ring becomes energetically accessible, enforcing association between the two components and hence decreasing the fluorescence output of the BODIPY rotor. The ultrafast, photoinduced electron transfer from the BODIPY rotor to the CBPQT^{4+} ring in MeCN is corroborated by femtosecond transient absorption (fsTA) spectroscopy, which reveals the characteristic absorption features of the reduced CBPQT^{4+} ring. The unconventional electrochromic behavior of the fluorescent molecular rotor embedded within this bistable [2]rotaxane, generated by the mechanical motion of the redox-actuated switching process, demonstrates that mechanical bonding remains a powerful strategy to create unpredictable emergent properties in MIMs through the induced nano-

https://dx.doi.org/10.1021/jacs.0c03701
J. Am. Chem. Soc. 2020, 142, 11835−11846

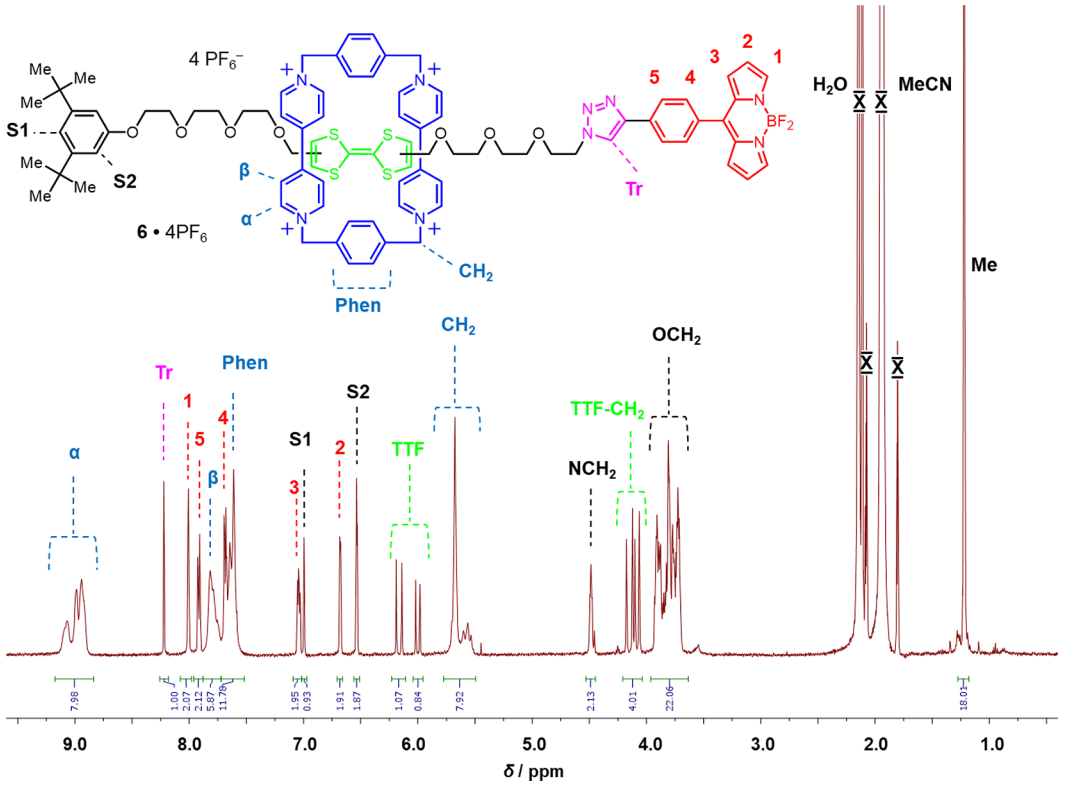

Figure 1. ^{1}H NMR spectrum (600 MHz, CD_3CN, 298 K) of bistable [2]rotaxane **6**·4PF_6.

confinement effect. This electrochemically addressable fluorescent bistable rotaxane is of particular interest for the development of electro-optical applications because, in contrast with conventional electro-optical molecular switches, the change in fluorescence output in the rotaxane-based system is modulated by mechanical movement within the MIM, which can lead to more sophisticated outcomes.

RESULTS AND DISCUSSION

Synthesis and NMR Spectroscopy. The 1,3-dipolar cycloadditions[21] of azides with alkynes, otherwise known as the copper-catalyzed azide−alkyne cycloaddition (CuAAC) approach to synthesis, has been demonstrated[22] to be highly effective when employed in the final step, leading to formation of mechanical bonds in the syntheses of MIMs, such as rotaxanes. The CuAAC reaction occurs readily under very mild conditions and at room temperature, a quality that is desirable for the template-directed synthesis of MIMs on account of optimal stabilization of the supramolecular intermediates.

TTF and its derivatives have been used widely in the design and synthesis of reversible, electrochemically switchable, supramolecular systems[23] and MIMs.[24,25] The π-electron-rich neutral TTF can be oxidized in two steps at mild potentials to give a stable radical cation and dication, respectively. In its neutral state, the TTF unit is bound strongly[23a] inside the π-electron-poor $CBPQT^{4+}$. Oxidation, however, leads to ejection of the oxidized TTF^{2+} dication from inside the tetracationic cyclophane as a consequence of Coulombic repulsions.

The BODIPY-alkyne **4**, which was synthesized following a method reported in the literature by Wagner and Lindsey,[26] was obtained (Scheme 2) in four steps. As for the synthesis of the *meso*-substituted dipyrromethanes **2**, we adopted a one-flask synthesis, which was developed previously for preparation of trans-substituted porphyrins.[27] Pyrroles readily undergo acid-catalyzed condensation at room temperature in the presence of highly electrophilic carbonyl compounds, such as aldehyde **1**, which is used to form the *meso* bridge.[28] In order to avoid oligomerization, a large excess of pyrrole is employed. Moreover, pyrrole serves as the solvent for the reaction, leading to direct formation of dipyrromethane **2**.

The π-electron-rich TTF derivative **5** was prepared using a previously reported procedure.[29] Upon mixing of **5** with 1 mol equiv of CBPQT·4PF_6 in Me_2CO, the solution immediately turned an intense emerald green color, indicating formation of a donor−acceptor pseudorotaxane complex, namely, [**5**⊂CBPQT]·4PF_6. Reaction with tetrakis(acetonitrile)copper(I) hexafluorophosphate in the presence of tris[(1-benzyl-1*H*-1,2,3-triazol-4-yl)methyl]amine (TBTA) at 20 °C for 5 days promoted the desired click reaction, affording the bistable [2]rotaxane **6**·4PF_6 as a dark green solid in 20% yield. Reference dumbbell compound **DB** was obtained (Scheme 2) under similar reaction conditions in the absence of **CBPQT**·4PF_6. The molecular structures and compound purities were ascertained by mass spectrometry and HPLC as well as by 1D and 2D NMR spectroscopies. See the Supporting Information (SI) for detailed synthetic procedures and characterization.

The ^{1}H NMR spectrum (Figure 1) of **6**·4PF_6 confirms its mechanically interlocked nature and the fact that the $CBPQT^{4+}$ ring encircles the TTF unit in the ground state. Notably, the separation of the signals for both the α- and the β-bipyridinium protons on the $CBPQT^{4+}$ ring is observed at room temperature. This observation is to be expected, as the constitutional asymmetry of the dumbbell component imposes its lack of symmetry on the $CBPQT^{4+}$ ring, rendering the α- and β-bipyridinium protons heterotopic and thus, in each case, giving rise to separate signals. We were not able to observe (Figure S8, Supporting Information) any ground-state

https://dx.doi.org/10.1021/jacs.0c03701
J. Am. Chem. Soc. 2020, 142, 11835−11846

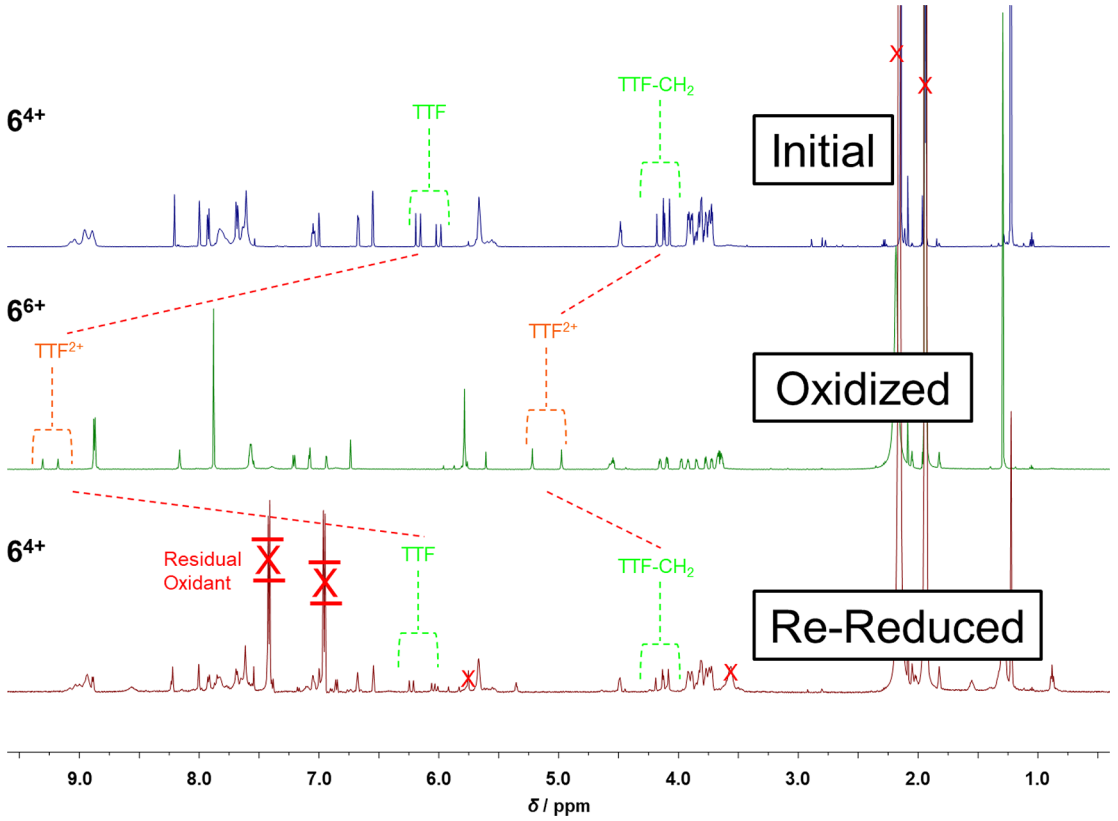

Figure 2. ^{1}H NMR spectra (600 MHz, CD_3CN, 298 K) of the bistable [2]rotaxane $\mathbf{6}^{4+}$, fully oxidized $\mathbf{6}^{6+}$ after addition of 2 equiv of the chemical oxidant tris(4-bromophenyl)ammoniumyl hexachloroantimonate, and rereduced $\mathbf{6}^{4+}$ after addition of Zn dust. Resonances due to the chemical oxidant and residual solvent are marked with red (X) symbols.

shuttling by dynamic ^{1}H NMR spectroscopy within the temperature range from 238 to 308 K, indicating that the $CBPQT^{4+}$ ring resides, to all intents and purposes, solely on the TTF unit, at least within the limits of detection provided by variable-temperature ^{1}H NMR spectroscopy. This observation is consistent with the one-station nature of the bistable [2]rotaxane when the TTF unit is neutral.

The bistable [2]rotaxane $\mathbf{6}\cdot 4PF_6$ can be actuated (Scheme 1) by chemical oxidation of $\mathbf{6}^{4+}$ to $\mathbf{6}^{6+}$ in CD_3CN using 2 equiv of tris(4-bromophenyl)ammoniumyl hexachloroantimonate as an oxidizing agent.[30] The effects of chemical switching can be monitored by ^{1}H NMR spectroscopy, steady-state UV−vis absorption, and emission spectroscopy. The ^{1}H NMR spectrum of $\mathbf{6}^{6+}$ (Figure 2) is characterized by a substantial change as a consequence of large downfield shifts of the TTF^{2+} proton resonances as well as those associated with the neighboring methylene groups. These changes are in agreement with previously reported[31] spectroscopic data. Before oxidation, the spectrum of bistable rotaxane $\mathbf{6}^{4+}$ reveals two pairs of peaks of almost equal integration (56:44), at δ = 6.19 and 6.14 ppm and δ = 6.02 and 5.98 ppm, which can be assigned to the constitutionally heterotopic TTF methine protons in the cis and trans isomers, respectively. These isomers are in dynamic equilibrium on the laboratory time scale. Following oxidation, the signals for the constitutionally heterotopic methine protons on the TTF^{2+} dication resonate[32] at δ = 9.30 and 9.17 ppm, while those associated with the methylene protons on the adjacent CH_2 groups are shifted downfield to 5.21 and 4.96 ppm. In this oxidized state, cis−trans isomerism is removed since the TTF^{2+} dication is no longer planar.[30a] The movement of the $CBPQT^{4+}$ ring from the TTF unit to the BODIPY rotor was probed (Figures S9 and S10) by two-dimensional (2D) nuclear Overhauser effect (NOE) measurements, where the presence of through-space correlations between the resonances for the BODIPY protons and those on the $CBPQT^{4+}$ ring in $\mathbf{6}^{6+}$ were observed. It should be noted that the interaction between the $CBPQT^{4+}$ ring and the BODIPY rotor was absent in the reduced $\mathbf{6}^{4+}$ state. The disappearance of NOE correlations between the methylene protons next to the TTF unit and those of the $CBPQT^{4+}$ ring corroborates the switching to $\mathbf{6}^{6+}$. Upon treatment with Zn dust, TTF^{2+} was reduced (Figure 2) to its neutral form and the $CBPQT^{4+}$ ring moved back to reside on the π-electron-rich TTF unit, as indicated by the ^{1}H NMR spectrum of the product, in order to re-establish the CT interactions between TTF and the $CBPQT^{4+}$ ring.

Steady-State UV−vis Spectroscopy. The UV−vis absorption spectrum (Figure 3a, green trace) of the bistable [2]rotaxane $\mathbf{6}\cdot 4PF_6$ shows the characteristic charge-transfer (CT) absorption band[33] centered on 843 nm (ε = 3500 M^{-1} cm^{-1}) for the TTF unit residing inside the $CBPQT^{4+}$ ring. Furthermore, in the visible region, the strong absorption band at 499 nm (ε = 48 000 M^{-1} cm^{-1}), typical of an $S_1 \leftarrow S_0$ electronic transition of the BODIPY chromophore unit, is observed. The UV region is characterized by the $S_2 \leftarrow S_0$ transition of BODIPY (376 nm, ε = 16 000 M^{-1} cm^{-1}) and the $CBPQT^{4+}$ absorption at 260 nm (ε = 40 000 M^{-1} cm^{-1}). Switching of $\mathbf{6}^{4+}$ was investigated in a 6.25 μM solution of the $4PF_6^-$ salt in MeCN when $Fe(ClO_4)_3$ was added.[34] Addition of 1 mol equiv of this chemical oxidant led (Figure 3a, orange trace) to disappearance of the CT absorption band at 843 nm and the rise of absorption bands centered on 450 and 600 nm

https://dx.doi.org/10.1021/jacs.0c03701
J. Am. Chem. Soc. 2020, 142, 11835−11846

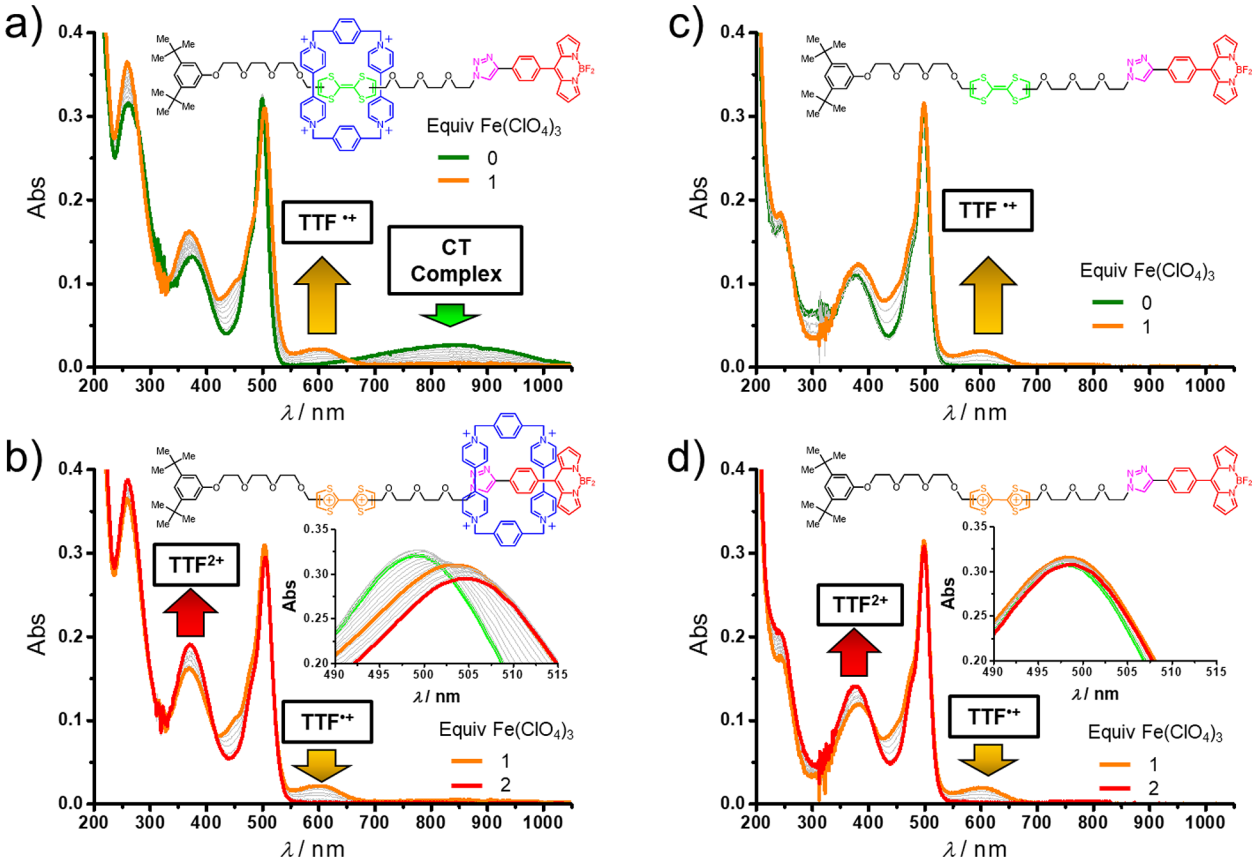

Figure 3. UV−vis absorption spectra of (a and b) the bistable [2]rotaxane **6**·4PF$_6$ and (c and d) the reference dumbbell **DB** in MeCN (6.25 μM, 10 mm optical pathway) following addition of Fe(ClO$_4$)$_3$ as the chemical oxidant.

characteristic[35] of the mono-oxidized form of the TTF. Further addition of the oxidant (up to 2 mol equiv) led to disappearance of the absorption bands for the mono-oxidized TTF unit and enhancement of the band at 375 nm (Figure 3b, red trace), indicative[35] of TTF^{2+} dication formation. Notably, movement of the CBPQT^{4+} ring away from the TTF unit is also accompanied by a small red shift of the absorption maximum of BODIPY from 499 to 505 nm. This observed ground-state electronic perturbation is most likely caused by the enforced encirclement of the BODIPY rotor by the tetracationic cyclophane, as reference **DB** does not show (Figure 3c and 3d) any red shift upon oxidation of the TTF unit. After reduction with Zn powder, the original spectrum is quantitatively restored. In summary, both the ^{1}H NMR spectroscopic and the UV−vis spectrophotometric experiments showed clearly that redox switching of the TTF unit forces the CBPQT^{4+} ring toward and away from the BODIPY rotor.

Electrochemistry. Switching of the bistable [2]rotaxane can also be enacted electrochemically. The CBPQT^{4+} ring shows (Figure 4a) two characteristic reversible two-electron reductions with $E_{1/2}$ at −270 and −715 mV vs Ag/AgCl, while the BODIPY rotor reveals (Figure 4b) a reversible one-electron reduction at $E_{1/2}$ = −652 mV and an irreversible oxidation peak at +1630 mV. The TTF oxidation processes, which are TTF → TTF$^{\bullet+}$ followed by TTF$^{\bullet+}$ → TTF^{2+} one-electron events, are well resolved in the CV of **DB** (Figure 4c) with $E_{1/2}$ at +392 and +755 mV, respectively. On the other hand, the oxidative scan of the bistable [2]rotaxane **6**·4PF$_6$ (Figure 4d) shows only one peak centered at +772 mV encompassing both of the one-electron processes, which together generate the TTF^{2+} dicationic state from its neutral form to the radical TTF$^{\bullet+}$ intermediate. Complete disappearance of the first oxidation peak matches the fact that the TTF unit within the bistable [2]rotaxane **6**·4PF$_6$ is encircled completely by the electron-poor CBPQT^{4+} ring, such that the first TTF oxidation is shifted substantially to a more positive potential, close to the potential for the second oxidation.[13] We also performed variable scan-rate CV measurements in order to elucidate the kinetics associated with the return of the CBPQT^{4+} ring from the oxidation-induced coconformation to the ground-state coconformation (GSCC). As observed in other bistable MIMs,[24e] the initial oxidation of the TTF unit forces the CBPQT^{4+} ring onto the alternative recognition site, and the subsequent rereduction of the TTF unit back to its neutral form does not result immediately in the regeneration of the GSCC. The transient coconformation, where the CBPQT^{4+} ring still encircles the weaker binding site while the TTF unit is back in the neutral state, is referred to as the metastable-state coconformation (MSCC). As the conversion of the MSCC to the GSCC is usually an activated process, its kinetics have a measurable rate, from seconds to hours, which depends on the nature of the linker, the temperature, and the environment.[31] In the case of the bistable [2]rotaxane **6**$^{4+}$, however, even at a high scan rate (2000 mV/s, Figure S11), we could not detect the presence of any MSCC, which would appear as emergence of the first oxidation of free TTF in the second scan. The absence of any detectable MSCC suggests that there is not much, if any, affinity between the CBPQT^{4+} ring and the BODIPY rotor,

https://dx.doi.org/10.1021/jacs.0c03701
J. Am. Chem. Soc. 2020, 142, 11835−11846

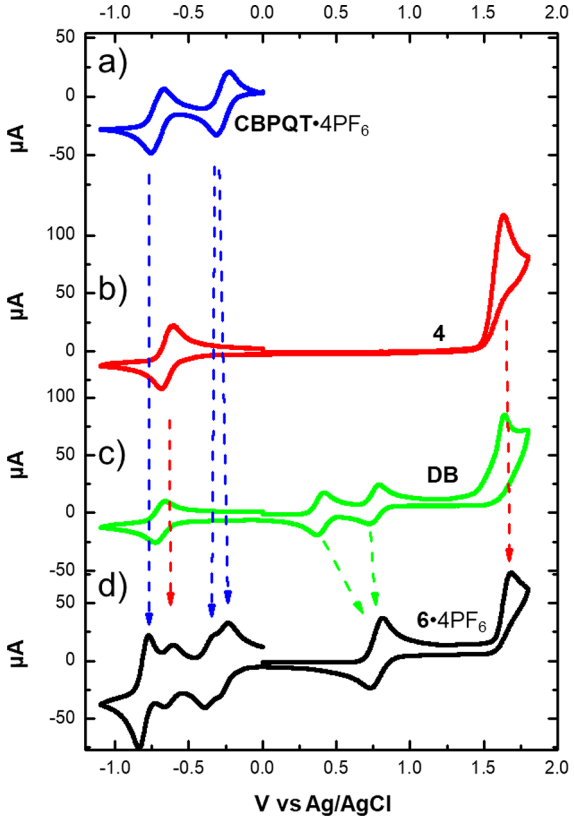

Figure 4. Cyclic voltammograms of (a) the ring component **CBPQT**·$4PF_6$, (b) the BODIPY-alkyne **4**, (c) the dumbbell **DB**, and (d) the bistable [2]rotaxane **6**·$4PF_6$.

and their association after the oxidation step is driven largely by the Coulombic repulsion between the tetracationic cyclophane and the TTF^{2+} dication.

Quantum Mechanical Calculations. In order to examine the energetics that govern the intramolecular noncovalent bonding interactions in the bistable [2]rotaxane **6**·$4PF_6$ in its different redox states, we performed density functional theory (DFT) calculations at the M06-2X/6-311++G**//M06-2X/6-31G* level that includes corrections for van der Waals attraction (normally not included in DFT).[36] Although $\mathbf{6}^{4+}$ has multiple rotatable C−O and C−C single bonds, we started with the linear conformation that has the longest possible distance between the TTF at the center and the two ends of $\mathbf{6}^{4+}$. This conformation minimizes the electrostatic repulsion between TTF^{2+} and $CBPQT^{4+}$ once TTF is oxidized and $CBPQT^{4+}$ is driven to one of the two ends. We assume that the entropic contribution to the free energy from the multiple rotatable single bonds will cancel out as $CBPQT^{4+}$ relocates. The ground-state geometries and energy landscapes predicted from the DFT methods (Figure 5), carried out on the $\mathbf{6}^{4+}$ and $\mathbf{6}^{6+}$ states, are in agreement with the experimental observations. In $\mathbf{6}^{4+}$ the $CBPQT^{4+}$ ring prefers to reside on the TTF unit rather than on the BODIPY rotor by 19.8 kcal/mol due to stronger donor−acceptor interactions between $CBPQT^{4+}$ and TTF. Once two electrons are removed from the TTF unit, the strong electrostatic repulsion between TTF^{2+} and $CBPQT^{4+}$ drives the ring to relocate preferentially beside the BODIPY rotor, leading to a 47.9 kcal/mol energy stabilization. The other coconformation of $\mathbf{6}^{6+}$ has the $CBPQT^{4+}$ ring move to the di-*tert*-butyl benzene unit, which is 10.0 kcal/mol higher in energy than when the $CBPQT^{4+}$ ring resides beside the BODIPY rotor.

Redox Modulation of Excited-State Properties. In order to demonstrate the ability of the bistable [2]rotaxane to modulate fluorescence outputs and excited-state dynamics of the BODIPY rotor, we performed steady-state fluorescence titration and fsTA measurements before and after chemical oxidation. A dilute solution of **6**·$4PF_6$ in PhMe excited at 467 nm shows (Figure 6a, green trace) the characteristic emission maximum of BODIPY around 520 nm. The measured fluorescence quantum yield is low (Φ_{em} = 0.19%) and insensitive to the solvent polarity, as observed (Figure 6b and 6c, green traces) in both MeCN and THF. These results are consistent[37] with those reported for sterically unhindered BODIPY derivatives. Upon addition of 2 mol equiv of $Fe(ClO_4)_3$, a 3.4-fold increase in fluorescence intensity was

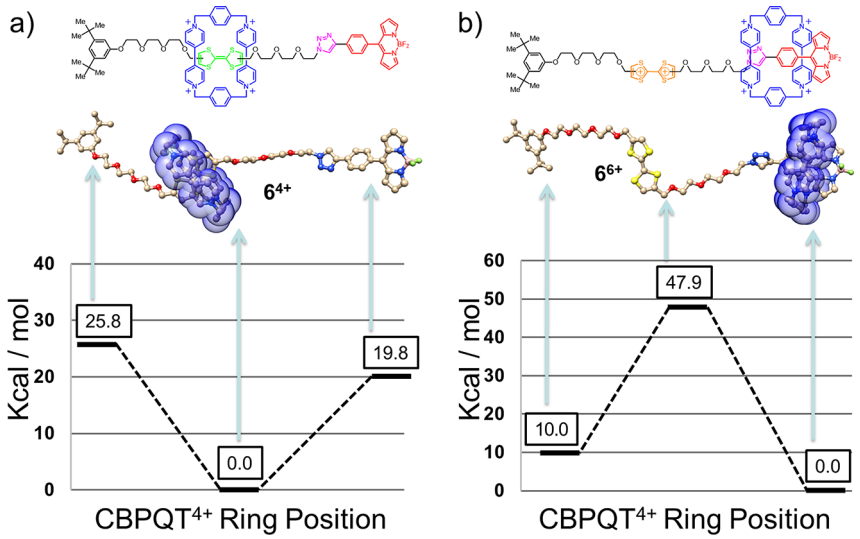

Figure 5. DFT-calculated relative energy surface diagrams of (a) $\mathbf{6}^{4+}$ and (b) $\mathbf{6}^{6+}$. Compound $\mathbf{6}^{4+}$ exists as a single ground-state coconformation. Oxidizing the TTF-containing dumbbell unit to afford $\mathbf{6}^{6+}$ dramatically increases the Columbic repulsion of TTF^{2+} with the $CBPQT^{4+}$ ring, causing it to translate wholly to the site located on the BODIPY unit.

https://dx.doi.org/10.1021/jacs.0c03701
J. Am. Chem. Soc. 2020, 142, 11835−11846

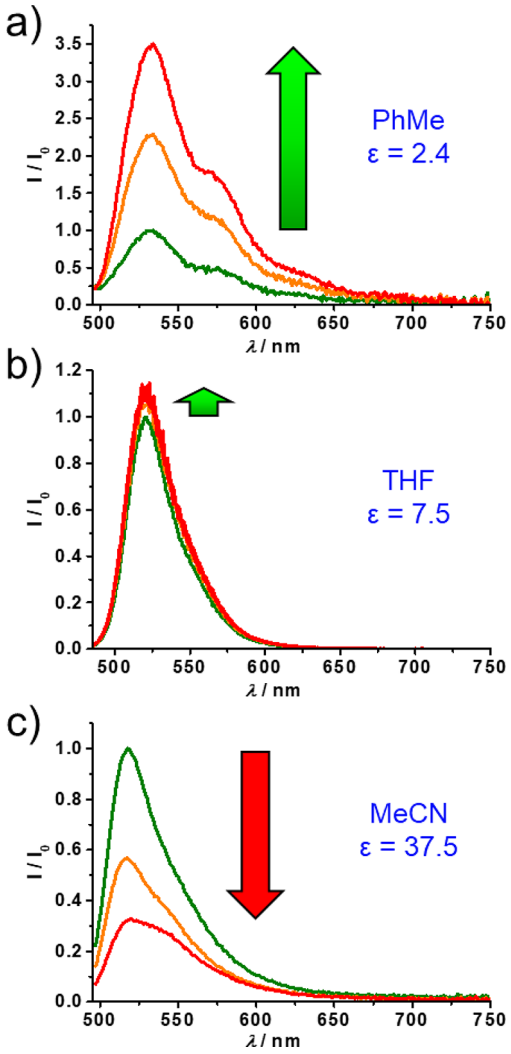

Figure 6. Fluorescence spectral changes of the bistable [2]rotaxane **6**·4PF_6 (green traces) in (a) PhMe, (b) THF, and (c) MeCN following addition of 1 equiv (orange traces) and 2 equiv (red traces) of $Fe(ClO_4)_3$ as the chemical oxidant.

observed for $\mathbf{6}^{6+}$ in PhMe. For comparison, the fluorescence signal of the BODIPY unit in the reference dumbbell **DB**, measured (Figure S12) before and after oxidation of the TTF unit, does not show an appreciable change in the tested solvents. We attribute the fluorescence signal enhancement of the oxidized bistable [2]rotaxane to the expected increase in the energy barrier for intramolecular rotation of the BODIPY rotor induced by the enforced positioning of the $CBPQT^{4+}$ ring close to the rotor in the $\mathbf{6}^{6+}$ state. Unexpectedly, when the same fluorescence titration experiment of the bistable [2]-rotaxane is performed in MeCN (Figure 6c), a nearly 3-fold decrease in the fluorescence quantum yield is observed. In THF (Figure 6b), which has an intermediate polarity compared to PhMe and MeCN, neither an increase nor a decrease in the fluorescence signal is observed upon addition of $Fe(ClO_4)_3$. The different fluorescence responses of [2]rotaxane **6**·4PF_6, upon chemical switching in the three solvents, suggests that an additional excited-state reaction, which is highly sensitive to the solvent polarity, must be involved. We hypothesize that the quenching of fluorescence in MeCN could be indicative of a photoinduced electron-transfer reaction from the BODIPY singlet excited state to the electron-accepting $CBPQT^{4+}$ ring. In order to obtain support for this hypothesis, we performed fsTA spectroscopic investigations.

Photoexcitation of the bistable [2]rotaxane **6**·4PF_6 in MeCN at 497 nm with a 150 fs laser pulse populated the lowest excited singlet state of the BODIPY rotor, which displays a prominent ground-state bleach (GSB) at 500 nm and overlaps partially with stimulated emission (SE) signals in the 500−600 nm region (Figure 7a). These transient features decay biexponentially with time constants of $\tau_{S1^*\rightarrow S1}$ = 4.1 ± 0.3 ps and $\tau_{S1\rightarrow S0}$ = 31.7 ± 0.6 ps. The first decay component can be assigned to the solvation evolution or vibrational/conformational relaxation associated with the BODIPY core in the excited state, while the relaxed excited singlet state decays with the slower time constant to the ground state. On the other hand, photoexcitation of the oxidized [2]rotaxane $\mathbf{6}^{6+}$ under the same conditions generates ^{1}*BODIPY, which decays rapidly (τ_{CS} = 1.4 ± 0.3 ps) to produce (Figure 7c) a new species with an absorption maximum at 610 nm that is indicative[38] of the presence of the $CBPQT^{3+\bullet}$ (Figure S14). The free-energy change for such a process in polar MeCN can be estimated as $\Delta G_{CS} = e(E_{OX} - E_{RED}) - E_S$, where E_{OX} is the oxidation potential (+1.63 V, Figure 4) of the BODIPY rotor and E_{RED} is the reduction potential (−0.27 V, Figure 4) of the $CBPQT^{4+}$, while E_S is the energy of ^{1}*BODIPY (+2.44 eV, from the average of absorption and fluorescence maxima), so that ΔG_{CS} = −0.54 eV, and is thus consistent with the observed fluorescence-quenching results. The ΔG_{IP} for formation of an ion pair in a solvent of arbitrary polarity can be determined using an expression developed by Weller:[39]

$$\Delta G_{IP} = e(E_{OX} - E_{RED}) + \frac{3e^2}{4\pi\varepsilon_0\varepsilon_s r_{12}} + \frac{e^2}{4\pi\varepsilon_0}\left(\frac{1}{2r_D} + \frac{1}{2r_A}\right)\left(\frac{1}{\epsilon_s} - \frac{1}{\epsilon_{sp}}\right) \quad (1)$$

where the redox potentials are measured in a high-polarity solvent with a static dielectric constant ε_{sp}, e is the charge of the electron, r_{12} is the ion-pair distance, r_D and r_A are the ionic radii, and ε_s is the static dielectric constant of a solvent of arbitrary polarity. While the term involving the ion-pair distance is the Coulombic interaction of the ions, the last term accounts for the lesser ability of the lower-polarity solvents to stabilize charges as compared to the higher polarity used in the electrochemical measurements. There are several limitations, however, with this treatment for estimating ΔG_{IP} for large π-stacked donor−acceptor systems. First, the ionic radii of the donor and acceptor are larger than the distance between them, which violates the assumption of a hard-sphere model surrounded by a continuous dielectric that is intrinsic to eq 1. Second, the BODIPY unit is highly shielded from the surrounding medium by the presence of the $CBPQT^{4+}$ ring; thus, BODIPY experiences a significant electrostatic influence from the $CBPQT^{4+}$ ring, which will deviate from that of the bulk solvent. Nevertheless, one can estimate that the energy of the CS state is destabilized by at least 0.6 eV in PhMe relative to its energy in MeCN, making the photoinduced electron-transfer reaction endoenergetic by ≥0.1 eV.[40] Notably, the charge recombination proceeds biexponentially. The shorter lifetime (8.0 ± 0.3 ps) can be safely assigned to the geminate recombination from $TTF-CBPQT^{3+\bullet}-BODIPY^{+\bullet}$ to the ground state. A smaller fraction of the population, however, can undergo to a charge-shift reaction to generate $TTF^{+\bullet}-$

https://dx.doi.org/10.1021/jacs.0c03701
J. Am. Chem. Soc. 2020, 142, 11835−11846

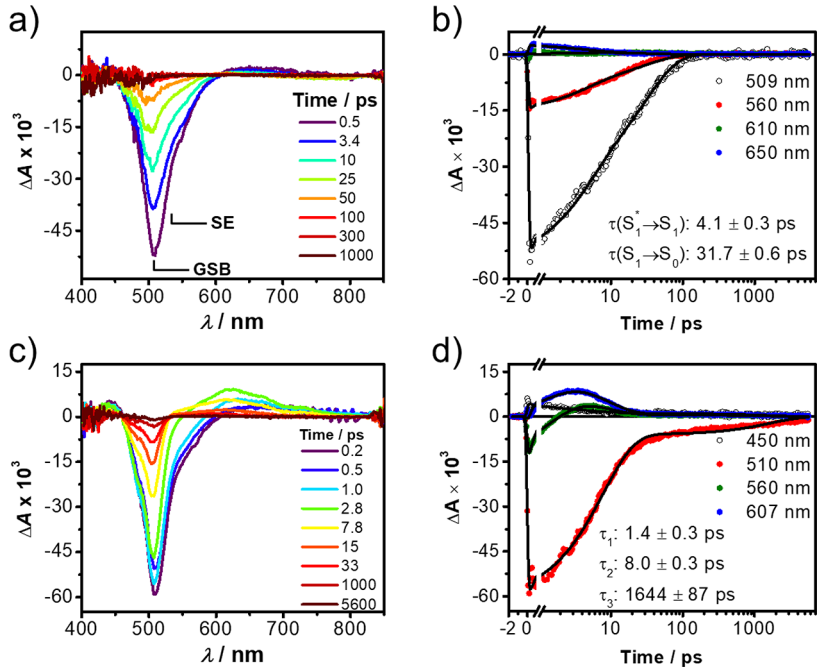

Figure 7. fsTA spectroscopy of the bistable [2]rotaxane **6**·4PF$_6$ in MeCN (a and b) before and (c and d) after addition of 2 equiv of Fe(ClO$_4$)$_3$ as the chemical oxidant. Samples were excited at 497 nm with a ∼150 fs laser pulse. (a and c) fsTA spectra at selected delay times; (b and d) kinetic fits at selected wavelengths.

CBPQT^{4+}–BODIPY$^{+\bullet}$, which ultimately decays in 1644 ± 87 ps. The energy levels and excited-state decay pathways under various conditions are summarized in Figure 8.

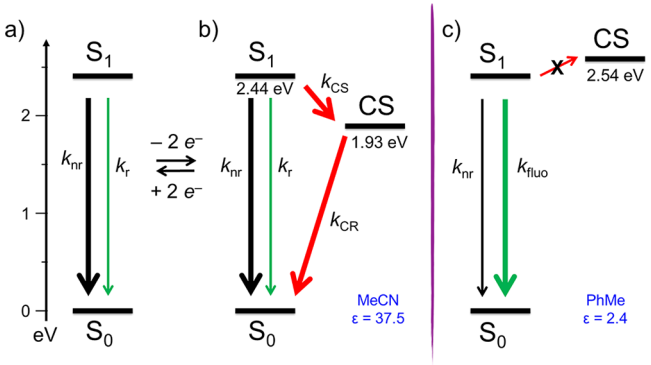

Figure 8. Energy diagram showing excited-state decay pathways of the bistable [2]rotaxane **6**·4PF$_6$ in MeCN (a) before and (b) after the addition of 2 equiv of Fe(ClO$_4$)$_3$ as the chemical oxidant. In a low-polarity solvent such as PhMe (c), the photoinduced electron-transfer reaction is energetically unfavorable and the fluorescence decay is enhanced on account of the hindered intramolecular binding rotation responsible for the nonradiative decay process.

CONCLUSIONS

We have reported the synthesis of an electrochemically switchable bistable [2]rotaxane with an embedded fluorescent molecular rotor, the BODIPY rotor, and demonstrated that the redox actuation of this mechanically interlocked molecule can impose a nanoconfined constrained environment that controls the rotation of the fluorescent rotor, resulting in a unique electrochromic effect. The electrochemically switchable [2]-rotaxane, **6**·4PF$_6$, composed of a CBPQT^{4+} ring mechanically interlocked with a dumbbell component containing a TTF recognition site and a functional fluorescent molecular rotor in the form of a BODIPY stopper, was synthesized in good yield by a template-directed protocol utilizing a "threading-followed-by-stoppering" approach in combination with the CuAAC reaction. The bistable [2]rotaxane can be switched reversibly so that the CBPQT^{4+} ring is positioned next to the BODIPY rotor upon oxidation of the TTF unit to its TTF^{2+} dication. We investigated the switching of the ground-state coconformation by means of 1D and 2D NMR spectroscopies and investigated the corresponding electronic excited-state dynamics changes using a variety of steady-state and time-resolved optical spectroscopies. Remarkably, two completely different mechanisms of fluorescence coexist within this fluorescent-bistable rotaxane upon switching of its ground-state coconformation: (i) fluorescence enhancement by reducing the loss of energy from the excited states to the nonradiative molecular motions of the BODIPY rotor in low-polarity solvents and (ii) fluorescence quenching on account of the photoinduced electron-transfer reaction from the BODIPY singlet excited state to the electron-accepting CBPQT^{4+} ring in polar solvents. This electrochromic effect is generated by the constrained nanoconfined environment introduced by the mechanical bond in this bistable [2]rotaxane which imparts the forced association between the CBPQT^{4+} ring and the BODIPY rotor, driven purely by the Coulombic repulsion between the tetracationic ring and the TTF^{2+} dication on the dumbbell. We believe that the extension of the concept of the nanoconfinement effect,[20] introduced by mechanical bonding in the context of stimuli-responsive materials based on MIMs, could lead to novel electro-optical switchable materials that can perform complex operations, holding promise for future applications as sensors, molecular memories, and molecular logic gates.

https://dx.doi.org/10.1021/jacs.0c03701
J. Am. Chem. Soc. 2020, 142, 11835–11846

■ ASSOCIATED CONTENT

Supporting Information

The Supporting Information is available free of charge at https://pubs.acs.org/doi/10.1021/jacs.0c03701.

Experimental details, including synthesis, NMR, and supportive figures; additional electrochemical studies and fluorescence spectra; quantum mechanical calculations (PDF)

■ AUTHOR INFORMATION

Corresponding Authors

Marco Frasconi − *Department of Chemical Sciences, University of Padova, Padova 35131, Italy;* orcid.org/0000-0003-2010-175X; Email: marco.frasconi@unipd.it

Michael R. Wasielewski − *Department of Chemistry and Institute for Sustainability and Energy at Northwestern (ISEN), Northwestern University, Evanston, Illinois 60208, United States;* orcid.org/0000-0003-2920-5440; Email: m-wasielewski@northwestern.edu

J. Fraser Stoddart − *Department of Chemistry, Northwestern University, Evanston, Illinois 60208, United States; Institute for Molecular Design and Synthesis, Tianjin University, Tianjin 300072, China; School of Chemistry, University of New South Wales, Sydney, New South Wales 2052, Australia;* orcid.org/0000-0003-3161-3697; Email: stoddart@northwestern.edu

Authors

Yilei Wu − *Department of Chemistry, Northwestern University, Evanston, Illinois 60208, United States;* orcid.org/0000-0001-6756-1855

Wei-Guang Liu − *Materials and Process Simulation Center, California Institute of Technology, Pasadena, California 91125, United States;* orcid.org/0000-0002-6633-7795

Ryan M. Young − *Department of Chemistry, Northwestern University, Evanston, Illinois 60208, United States;* orcid.org/0000-0002-5108-0261

William A. Goddard III − *Materials and Process Simulation Center, California Institute of Technology, Pasadena, California 91125, United States;* orcid.org/0000-0003-0097-5716

Complete contact information is available at: https://pubs.acs.org/10.1021/jacs.0c03701

Notes

The authors declare no competing financial interest.

■ ACKNOWLEDGMENTS

The authors thank NU for their continued support of this research. Synthesis was supported by the National Science Foundation under CHE-1308107 (J.F.S.). This project was also supported by the U.S. Department of Energy, Office of Science, Office of Basic Energy Sciences under Award DE-FG02-99ER14999 (M.R.W.). W.-G.L. and W.A.G. were supported by NSF (CBET-1805022). Y.W. thanks the Fulbright Scholar Program for a Fellowship and the NU International Institute of Nanotechnology for a Ryan Fellowship. We thank the personnel in the Integrated Molecular Structure Education and Research Center (IMSERC) at Northwestern University (NU) for their assistance in the collection of the analytical data.

■ REFERENCES

(1) (a) Sauvage, J.-P. Transition Metal-Containing Rotaxanes and Catenanes in Motion: Toward Molecular Machines and Motors. *Acc. Chem. Res.* **1998**, *31*, 611−619. (b) Balzani, V.; Credi, A.; Raymo, F. M.; Stoddart, J. F. Artificial Molecular Machines. *Angew. Chem., Int. Ed.* **2000**, *39*, 3348−3391. (c) Browne, W. R.; Feringa, B. L. Making Molecular Machines Work. *Nat. Nanotechnol.* **2006**, *1*, 25−35. (d) Kay, E. R.; Leigh, D. A.; Zerbetto, F. Synthetic Molecular Motors and Mechanical Machines. *Angew. Chem., Int. Ed.* **2007**, *46*, 72−191. (e) Cacialli, F.; Wilson, J. S.; Michels, J. J.; Daniel, C.; Silva, C.; Friend, R. H.; Severin, N.; Samorì, P.; Rabe, J. P.; O'Connell, M. J.; Taylor, P. N.; Anderson, H. L. Cyclodextrin-Threaded Conjugated Polyrotaxanes as Insulated Molecular Wires with Reduced Interstrand Interactions. *Nat. Mater.* **2002**, *1*, 160−164. (f) Langton, M. J.; Beer, P. D. Rotaxane and Catenane Host Structures for Sensing Charged Guest Species. *Acc. Chem. Res.* **2014**, *47*, 1935−1949. (g) De Bo, G.; Gall, M. A. Y.; Kuschel, S.; De Winter, J.; Gerbaux, P.; Leigh, D. A. An Artificial Molecular Machine that Builds an Asymmetric Catalyst. *Nat. Nanotechnol.* **2018**, *13*, 381−385. (h) Chen, S.; Wang, Y.; Nie, T.; Bao, C.; Wang, C.; Xu, T.; Lin, Q.; Qu, D. H.; Gong, X.; Yang, Y.; Zhu, L.; Tian, H. An Artificial Molecular Shuttle Operates in Lipid Bilayers for Ion Transport. *J. Am. Chem. Soc.* **2018**, *140*, 17992−17998. (i) Corra, S.; de Vet, C.; Groppi, J.; La Rosa, M.; Silvi, S.; Baroncini, M.; Credi, A. Chemical On/Off Switching of Mechanically Planar Chirality and Chiral Anion Recognition in a [2]Rotaxane Molecular Shuttle. *J. Am. Chem. Soc.* **2019**, *141*, 9129−9133.

(2) (a) Bruns, C. J.; Stoddart, J. F. *The Nature of the Mechanical Bond: From Molecules to Machines*; Wiley: New York, 2017. (b) Stoddart, J. F. Mechanically Interlocked Molecules (MIMs)—Molecular Shuttles, Switches, and Machines (Nobel Lecture). *Angew. Chem., Int. Ed.* **2017**, *56*, 11094−11125.

(3) Liu, Y.; Flood, A. H.; Bonvallet, P. A.; Vignon, S. A.; Northrop, B. H.; Tseng, H.-R.; Jeppesen, J. O.; Huang, T. J.; Brough, B.; Baller, M.; Magonov, S.; Solares, S. D.; Goddard, W. A., III; Ho, C.-M.; Stoddart, J. F. Linear Artificial Molecular Muscles. *J. Am. Chem. Soc.* **2005**, *127*, 9745−9759.

(4) (a) Serreli, V.; Lee, C. F.; Kay, E. R.; Leigh, D. A. A Molecular Information Ratchet. *Nature* **2007**, *445*, 523−527. (b) Alvarez-Pérez, M.; Goldup, S. M.; Leigh, D. A.; Slawin, A. M. Z. A Chemically-Driven Molecular Information Ratchet. *J. Am. Chem. Soc.* **2008**, *130*, 1836−1838. (c) Carlone, A.; Goldup, S. M.; Lebrasseur, N.; Leigh, D. A.; Wilson, A. A Three-Compartment Chemically-Driven Molecular Information Ratchet. *J. Am. Chem. Soc.* **2012**, *134*, 8321−8323.

(5) (a) Koumura, N.; Zijlstra, R. W. J.; Van Delden, R. A.; Harada, N.; Feringa, B. L. Light-Driven Monodirectional Molecular Rotor. *Nature* **1999**, *401*, 152−155. (b) Leigh, D. A.; Wong, J. K. Y.; Dehez, F.; Zerbetto, F. Unidirectional Rotation in a Mechanically Interlocked Molecular Rotor. *Nature* **2003**, *424*, 174−179. (c) Wilson, M. R.; Solá, J.; Carlone, A.; Goldup, S. M.; Lebrasseur, N.; Leigh, D. A. An Autonomous Chemically Fuelled Small-Molecule Motor. *Nature* **2016**, *534*, 235−240. (d) Kassem, S.; van Leeuwen, T.; Lubbe, A. S.; Wilson, M. R.; Feringa, B. L.; Leigh, D. A. Artificial Molecular Motors. *Chem. Soc. Rev.* **2017**, *46*, 2592−2621.

(6) (a) Bissell, R. A.; Córdova, E.; Kaifer, A. E.; Stoddart, J. F. A Chemically and Electrochemically Switchable Molecular Shuttle. *Nature* **1994**, *369*, 133−137. (b) Anelli, P.-L.; Asakawa, M.; Ashton, P. R.; Bissell, R. A.; Clavier, G.; Górski, R.; Kaifer, A. E.; Langford, S. J.; Mattersteig, G.; Menzer, S.; Philp, D.; Slawin, A. M. Z.; Spencer, N.; Stoddart, J. F.; Tolley, M. S.; Williams, D. Toward Controllable Molecular Shuttles. *Chem. - Eur. J.* **1997**, *3*, 1113−1135. (c) Durola, F.; Sauvage, J.-P. Fast Electrochemically Induced Translation of the Ring in a Copper-Complexed [2]Rotaxane: The Biisoquinoline Effect. *Angew. Chem., Int. Ed.* **2007**, *46*, 3537−3540. (d) Nygaard, S.; Leung, K. C.-F.; Aprahamian, I.; Ikeda, T.; Saha, S.; Laursen, B. W.; Kim, S.-Y.; Hansen, S. W.; Stein, P. C.; Flood, A. H.; Stoddart, J. F.; Jeppesen, J. O. Functionally Rigid Bistable [2]-Rotaxanes. *J. Am. Chem. Soc.* **2007**, *129*, 960−970. (e) Andersen, S. S.; Share, A. I.; Poulsen, B. L.; Kørner, M.; Duedal, T.; Benson, C. R.; Hansen, S. W.; Jeppesen, J. O.; Flood, A. H. Mechanistic Evaluation

of Motion in Redox-Driven Rotaxanes Reveals Longer Linkers Hasten Forward Escapes and Hinder Backward Translations. *J. Am. Chem. Soc.* **2014**, *136*, 6373−6384.
(7) (a) Nishimura, D.; Oshikiri, T.; Takashima, Y.; Hashidzume, A.; Yamaguchi, H.; Harada, A. Relative Rotational Motion between α-Cyclodextrin Derivatives and a Stiff Axle Molecule. *J. Org. Chem.* **2008**, *73*, 2496−2502. (b) Yamauchi, K.; Miyawaki, A.; Takashima, Y.; Yamaguchi, H.; Harada, A. A Molecular Reel: Shuttling of a Rotor by Tumbling of a Macrocycle. *J. Org. Chem.* **2010**, *75*, 1040−1046. (c) Wang, Z.; Takashima, Y.; Yamaguchi, H.; Harada, A. Photoresponsive Formation of Pseudo[2]rotaxane with Cyclodextrin Derivatives. *Org. Lett.* **2011**, *13*, 4356−4359.
(8) (a) Baroncini, M.; Silvi, S.; Venturi, M.; Credi, A. Photoactivated Directionally Controlled Transit of a Non-Symmetric Molecular Axle Through a Macrocycle. *Angew. Chem., Int. Ed.* **2012**, *51*, 4223−4226. (b) Li, H.; Cheng, C.; McGonigal, P. R.; Fahrenbach, A. C.; Frasconi, M.; Liu, W.-G.; Zhu, Z.; Zhao, Y.; Ke, C. F.; Lei, J. Y.; Young, R. M.; Dyar, S. M.; Co, D. T.; Yang, Y. W.; Botros, Y. Y.; Goddard, W. A., III; Wasielewski, M. R.; Astumian, R. D.; Stoddart, J. F. Relative Unidirectional Translation in an Artificial Molecular Assembly Fueled by Light. *J. Am. Chem. Soc.* **2013**, *135*, 18609−18620. (c) Ragazzon, G.; Baroncini, M.; Silvi, S.; Venturi, M.; Credi, A. Light-Powered Autonomous and Directional Molecular Motion of a Dissipative Self-Assembling System. *Nat. Nanotechnol.* **2015**, *10*, 70−75.
(9) (a) Astumian, R. D.; Derényi, I. Fluctuation Driven Transport and Models of Molecular Motors and Pumps. *Eur. Biophys. J.* **1998**, *27*, 474−489. (b) Pezzato, C.; Cheng, C.; Stoddart, J. F.; Astumian, R. D. Mastering the Non-Equilibrium Assembly and Operation of Molecular Machines. *Chem. Soc. Rev.* **2017**, *46*, 5491−5507.
(10) Yu, J.-J.; Zhao, L.-Y.; Shi, Z.-T.; Zhang, Q.; London, G.; Liang, W.-J.; Gao, C.; Li, M.-M.; Cao, X.-M.; Tian, H.; Feringa, B. L.; Qu, D.-H. Pumping a Ring-Sliding Molecular Motion by a Light-Powered Molecular Motor. *J. Org. Chem.* **2019**, *84*, 5790−5802.
(11) (a) Kelly, T. R.; De Silva, H.; Silva, R. A. Unidirectional Rotary Motion in a Molecular System. *Nature* **1999**, *401*, 150−152. (b) Fletcher, S. P.; Dumur, F.; Pollard, M. M.; Feringa, B. L. A Reversible, Unidirectional Molecular Rotary Motor Driven by Chemical Energy. *Science* **2005**, *310*, 80−82.
(12) (a) Koumura, N.; Zijlstra, R. W. J.; van Delden, R. A.; Harada, N.; Feringa, B. L. Light-Driven Monodirectional Molecular Rotor. *Nature* **1999**, *401*, 152−155. (b) Wang, J. B.; Feringa, B. L. Dynamic Control of Chiral Space in a Catalytic Asymmetric Reaction Using a Molecular Motor. *Science* **2011**, *331*, 1429−1432. For a review, see: (c) Feringa, B. L. The Art of Building Small: From Molecular Switches to Molecular Motors. *J. Org. Chem.* **2007**, *72*, 6635−6652.
(13) For reviews on fluorescent molecular rotors, see: (a) Haidekker, M. A.; Theodorakis, E. A. Molecular Rotors—Fluorescent Biosensors for Viscosity and Flow. *Org. Biomol. Chem.* **2007**, *5*, 1669−1678. (b) Kuimova, M. K. Mapping Viscosity in Cells Using Molecular Rotors. *Phys. Chem. Chem. Phys.* **2012**, *14*, 12671−12686. (c) Lee, S. C.; Heo, J.; Woo, H. C.; Lee, J. A.; Seo, Y. H.; Lee, C. L.; Kim, S.; Kwon, O. P. Fluorescent Molecular Rotors for Viscosity Sensors. *Chem. - Eur. J.* **2018**, *24*, 13706−13718.
(14) Kuimova, M. K.; Yahioglu, G.; Levitt, J. A.; Suhling, K. Molecular Rotor Measures Viscosity of Live Cells via Fluorescence Lifetime Imaging. *J. Am. Chem. Soc.* **2008**, *130*, 6672−6673.
(15) (a) Li, F.; Yang, S. I.; Ciringh, Y.; Seth, J.; Martin, C. H., III; Singh, D. L.; Kim, D.; Birge, R. R.; Bocian, D. F.; Holten, D.; Lindsey, J. S. Design, Synthesis, and Photodynamics of Light-Harvesting Arrays Comprised of a Porphyrin and One, Two, or Eight Boron-Dipyrrin Accessory Pigments. *J. Am. Chem. Soc.* **1998**, *120*, 10001−10017. (b) Kee, H. L.; Kirmaier, C.; Yu, L. H.; Thamyongkit, P.; Youngblood, W. J.; Calder, M. E.; Ramos, L.; Noll, B. C.; Bocian, D. F.; Scheidt, W. R.; Birge, R. R.; Lindsey, J. S.; Holten, D. Structural Control of the Photodynamics of Boron-Dipyrrin Complexes. *J. Phys. Chem. B* **2005**, *109*, 20433−20443.
(16) Wu, Y. L.; Stefl, M.; Olzynska, A.; Hof, M.; Yahioglu, G.; Yip, P.; Casey, D. R.; Ces, O.; Humpolickova, J.; Kuimova, M. K. Molecular Rheometry: Direct Determination of Viscosity in L_o and L_d Lipid Phases via Fluorescence Lifetime Imaging. *Phys. Chem. Chem. Phys.* **2013**, *15*, 14986−14993.
(17) Dora Tang, T-Y.; Rohaida Che Hak, C.; Thompson, A. J.; Kuimova, M. K.; Williams, D. S.; Perriman, A. W.; Mann, S. Fatty Acid Membrane Assembly on Coacervate Microdroplets as a Step Towards a Hybrid Protocell Model. *Nat. Chem.* **2014**, *6*, 527−533.
(18) Lopez-Duarte, I.; Vu, T. T.; Izquierdo, M. A.; Bull, J. A.; Kuimova, M. K. A Molecular Rotor for Measuring Viscosity in Plasma Membranes of Live Cells. *Chem. Commun.* **2014**, *50*, 5282−5284.
(19) Levitt, J. A.; Chung, P. H.; Kuimova, M. K.; Yahioglu, G.; Wang, Y.; Qu, J. L.; Suhling, K. Fluorescence Anisotropy of Molecular Rotors. *ChemPhysChem* **2011**, *12*, 662−672.
(20) Grommet, A. B.; Feller, M.; Klajn, R. Chemical Reactivity Under Nanoconfinement. *Nat. Nanotechnol.* **2020**, *15*, 256−271.
(21) (a) Huisgen, R. 1,3-Dipolar Cycloadditions. Past and Future. *Angew. Chem., Int. Ed. Engl.* **1963**, *2*, 565−598. (b) Rostovtsev, V. V.; Green, L. G.; Fokin, V. V.; Sharpless, K. B. A Stepwise Huisgen Cycloaddition Process: Copper(I)-Catalyzed Regioselective "Ligation" of Azides and Terminal Alkynes. *Angew. Chem., Int. Ed.* **2002**, *41*, 2596−2599. (c) Meldal, M.; Tornøe, C. W. Cu-Catalyzed Azide−Alkyne Cycloaddition. *Chem. Rev.* **2008**, *108*, 2952−3015.
(22) (a) Dichtel, W. R.; Miljanić, O. Š.; Spruell, J. M.; Heath, J. R.; Stoddart, J. F. Efficient Templated Synthesis of Donor−Acceptor Rotaxanes Using Click Chemistry. *J. Am. Chem. Soc.* **2006**, *128*, 10388−10390. (b) Dichtel, W. R.; Miljanić, O. Š.; Zhang, W.; Spruell, J. M.; Patel, K.; Aprahamian, I.; Heath, J. R.; Stoddart, J. F. Kinetic and Thermodynamic Approaches for the Efficient Formation of Mechanical Bonds. *Acc. Chem. Res.* **2008**, *41*, 1750−1761. (c) Hänni, K. D.; Leigh, D. A. The Application of CuAAC 'Click' Chemistry to Catenane and Rotaxane Synthesis. *Chem. Soc. Rev.* **2010**, *39*, 1240−1251.
(23) (a) Jeppesen, J. O.; Nielsen, M. B.; Becher, J. Tetrathiafulvalene Cyclophanes and Cage Molecules. *Chem. Rev.* **2004**, *104*, 5115−5131. (b) Ziganshina, A. Y.; Ko, Y. H.; Jeon, W. S.; Kim, K. Stable π-Dimer of a Tetrathiafulvalene Cation Radical Encapsulated in the Cavity of Cucurbit[8]uril. *Chem. Commun.* **2004**, 806−807. (c) Yoshizawa, M.; Kumazawa, K.; Fujita, M. Room-Temperature and Solution-State Observation of the Mixed-Valence Cation Radical Dimer of Tetrathiafulvalene, $[(TTF)_2]^{+\bullet}$, within a Self-Assembled Cage. *J. Am. Chem. Soc.* **2005**, *127*, 13456−13457. (d) Canevet, D.; Salle, M.; Zhang, G.; Zhang, D.; Zhu, D. Tetrathiafulvalene (TTF) Derivatives: Key Building-Blocks for Switchable Processes. *Chem. Commun.* **2009**, 2245−2269. (e) Kim, D. S.; Chang, J.; Leem, S.; Park, J. S.; Thordarson, P.; Sessler, J. L. Redox- and pH-Responsive Orthogonal Supramolecular Self-Assembly: An Ensemble Displaying Molecular Switching Characteristics. *J. Am. Chem. Soc.* **2015**, *137*, 16038−16042. (f) Park, J. S.; Sessler, J. L. Tetrathiafulvalene (TTF)-Annulated Calix[4]pyrroles: Chemically Switchable Systems with Encodable Allosteric Recognition and Logic Gate Functions. *Acc. Chem. Res.* **2018**, *51* (10), 2400−2410.
(24) (a) Asakawa, M.; Ashton, P. R.; Balzani, V.; Credi, A.; Hamers, C.; Mattersteig, G.; Montalti, M.; Shipway, A. N.; Spencer, N.; Stoddart, J. F.; Tolley, M. S.; Venturi, M.; White, A. J. P.; Williams, D. J. A Chemically and Electrochemically Switchable [2]Catenane Incorporating a Tetrathiafulvalene Unit. *Angew. Chem., Int. Ed.* **1998**, *37*, 333−337. (b) Jeppesen, J. O.; Perkins, J.; Becher, J.; Stoddart, J. F. Slow Shuttling in an Amphiphilic Bistable [2]Rotaxane Incorporating a Tetrathiafulvalene Unit. *Angew. Chem., Int. Ed.* **2001**, *40*, 1216−1221. (c) Aprahamian, I.; Olsen, J.-C.; Trabolsi, A.; Stoddart, J. F. Tetrathiafulvalene Radical Cation Dimerization in a Bistable Tripodal [4]Rotaxane. *Chem. - Eur. J.* **2008**, *14*, 3889−3895. (d) Wang, C.; Dyar, S. M.; Cao, D.; Fahrenbach, A. C.; Horwitz, N.; Colvin, M. T.; Carmieli, R.; Stern, C. L.; Dey, S. K.; Wasielewski, M. R.; Stoddart, J. F. Tetrathiafulvalene Hetero Radical Cation Dimerization in a Redox-Active [2]Catenane. *J. Am. Chem. Soc.* **2012**, *134* (46), 19136−19145. (e) Fahrenbach, A. C.; Bruns, C. J.; Cao, D.; Stoddart, J. F. Ground-State Thermodynamics of Bistable Redox-Active Donor−Acceptor Mechanically Interlocked Molecules. *Acc. Chem. Res.* **2012**, *45*, 1581−1592.

https://dx.doi.org/10.1021/jacs.0c03701
J. Am. Chem. Soc. 2020, 142, 11835−11846

(25) (a) Spruell, J. M.; Coskun, A.; Friedman, D. C.; Forgan, R. S.; Sarjeant, A. A.; Trabolsi, A.; Fahrenbach, A. C.; Barin, G.; Paxton, W. F.; Dey, S. K.; et al. Highly Stable Tetrathiafulvalene Radical Dimers in [3]Catenanes. *Nat. Chem.* **2010**, *2*, 870−879. (b) Frasconi, M.; Kikuchi, T.; Cao, D.; Wu, Y.; Liu, W.-G.; Dyar, S. M.; Barin, G.; Sarjeant, A. A.; Stern, C. L.; Carmieli, R.; Wang, C.; Wasielewski, M. R.; Goddard, W. A., III; Stoddart, J. F. Mechanical Bonds and Topological Effects in Radical Dimer Stabilization. *J. Am. Chem. Soc.* **2014**, *136*, 11011−11026.

(26) Wagner, R. W.; Lindsey, J. S. Boron-Dipyrromethene Dyes for Incorporation in Synthetic Multi-Pigment Light-Harvesting Arrays. *Pure Appl. Chem.* **1996**, *68*, 1373−1380.

(27) Lee, C.-H.; Lindsey, J. S. One-Flask Synthesis of *Meso*-Substituted Dipyrromethanes and their Application in the Synthesis of Trans-Substituted Porphyrin Building Blocks. *Tetrahedron* **1994**, *50*, 11427−11440.

(28) Lindsey, J. S.; Schreiman, I. C.; Hsu, H. C.; Kearney, P. C.; Marguerettaz, A. M. Rothemund and Adler-Longo Reactions Revisited: Synthesis of Tetraphenylporphyrins Under Equilibrium Conditions. *J. Org. Chem.* **1987**, *52*, 827−836.

(29) Avellini, T.; Li, H.; Coskun, A.; Barin, G.; Trabolsi, A.; Basuray, A. N.; Dey, S. K.; Credi, A.; Silvi, S.; Stoddart, J. F.; Venturi, M. Photoinduced Memory Effect in a Redox Controllable Bistable Mechanical Molecular Switch. *Angew. Chem., Int. Ed.* **2012**, *51*, 1611−1615.

(30) For a description of the oxidizing agent, tris(4-bromophenyl) ammoniumyl hexachloroantimonate and its use in spectroscopic investigations, see: (a) Tseng, H.-R.; Vignon, S. A.; Stoddart, J. F. Toward Chemically Controlled Nanoscale Molecular Machinery. *Angew. Chem., Int. Ed.* **2003**, *42*, 1491−1495. For a review on this and other chemical oxidants commonly used in NMR spectroscopic investigations, see: (b) Connelly, N. G.; Geiger, W. E. Chemical Redox Agents for Organometallic Chemistry. *Chem. Rev.* **1996**, *96*, 877−910.

(31) Spruell, J. M.; Paxton, W. F.; Olsen, J.-C.; Benítez, D.; Tkatchouk, E.; Stern, C. L.; Trabolsi, A.; Friedman, D. C.; Goddard, W. A., III; Stoddart, J. F. A Push-Button Molecular Switch. *J. Am. Chem. Soc.* **2009**, *131*, 11571−11580.

(32) Ashton, P. R.; Balzani, V.; Becher, J.; Credi, A.; Fyfe, M. C. T.; Mattersteig, G.; Menzer, S.; Nielsen, M. B.; Raymo, F. M.; Stoddart, J. F.; Venturi, M.; Williams, D. J. A Three-Pole Supramolecular Switch. *J. Am. Chem. Soc.* **1999**, *121*, 3951−3957.

(33) Asakawa, M.; Ashton, P. R.; Balzani, V.; Credi, A.; Mattersteig, G.; Matthews, O. A.; Montalti, M.; Spencer, N.; Stoddart, J. F.; Venturi, M. Electrochemically Induced Molecular Motions in Pseudorotaxanes: A Case of Dual Mode (Oxidative and Reductive) Dethreading. *Chem. - Eur. J.* **1997**, *3*, 1992−1996.

(34) The chemical oxidant $Fe(ClO_4)_3$ was chosen for the UV−vis spectroscopic studies because it does not show any significant optical absorption band in the visible region, making changes in UV−vis absorption spectra easier to interpret.

(35) Hünig, S.; Kiesslich, G.; Quast, H.; Scheutzow, D. Über Zweistufige Redoxsysteme, X[1)] Tetrathio-Äthylene und Ihre Höheren Oxidationsstufen. *Liebigs Ann. Chem.* **1973**, *1973*, 310−323.

(36) Zhao, Y.; Truhlar, D. G. The M06 Suite of Density Functionals for Main Group Thermochemistry, Thermochemical Kinetics, Noncovalent Interactions, Excited States, and Transition Elements: Two New Functionals and Systematic Testing of Four M06-Class Functionals and 12 Other Functionals. *Theor. Chem. Acc.* **2008**, *120*, 215−241.

(37) (a) Alamiry, M. A. H.; Benniston, A. C.; Copley, G.; Elliott, K. J.; Harriman, A.; Stewart, B.; Zhi, Y. G. A Molecular Rotor Based on an Unhindered Boron Dipyrromethene (BODIPY) Dye. *Chem. Mater.* **2008**, *20*, 4024−4032. (b) Levitt, J. A.; Kuimova, M. K.; Yahioglu, G.; Chung, P. H.; Suhling, K.; Phillips, D. Membrane-Bound Molecular Rotors Measure Viscosity in Live Cells via Fluorescence Lifetime Imaging. *J. Phys. Chem. C* **2009**, *113*, 11634−11642.

(38) (a) Barnes, J. C.; Frasconi, M.; Young, R. M.; Khdary, N. H.; Liu, W. G.; Dyar, S. M.; McGonigal, P. R.; Gibbs-Hall, I. C.; Diercks, C. S.; Sarjeant, A. A.; Stern, C. L.; Goddard, W. A., III; Wasielewski, M. R.; Stoddart, J. F. Solid-State Characterization and Photoinduced Intramolecular Electron Transfer in a Nanoconfined Octacationic Homo[2]Catenane. *J. Am. Chem. Soc.* **2014**, *136*, 10569−10572. (b) Fernando, I. R.; Frasconi, M.; Wu, Y.; Liu, W. G.; Wasielewski, M. R.; Goddard, W. A., III; Stoddart, J. F. Sliding-Ring Catenanes. *J. Am. Chem. Soc.* **2016**, *138*, 10214−10225.

(39) (a) Weller, A. Z. Photoinduced Electron Transfer in Solution: Exciplex and Radical Ion Pair Formation Free Enthalpies and their Solvent Dependence. *Z. Phys. Chem.* **1982**, *133*, 93−98. (b) Young, R. M.; Dyar, S. M.; Barnes, J. C.; Juricek, M.; Stoddart, J. F.; Co, D. T.; Wasielewski, M. R. Ultrafast Conformational Dynamics of Electron Transfer in $ExBox^{4+} \subset$ Perylene. *J. Phys. Chem. A* **2013**, *117*, 12438−12448.

(40) Complementary fsTA measurements in PhMe, in an attempt to corroborate the excited-state dynamics, were unsuccessful because of the low solubility of both **6**·4PF_6 and **6**·6PF_6 in low-polarity solvents. Additional efforts to tune the polarity have been made using a binary solvent mixture of PhMe and MeCN (90:10 vol/vol). The fluorescence spectra, resulting from carrying out a titration experiment on the bistable [2]rotaxane in this solvent mixture, show (Figure S13) a decrease in the fluorescence upon addition of the oxidizing agent. This result might be, in part, related to a selective solvation effect of the bistable [2]rotaxane in the binary solvent system.

https://dx.doi.org/10.1021/jacs.0c03701
J. Am. Chem. Soc. 2020, 142, 11835−11846